Available online at www.sciencedirect.com
SCIENCE DIRECT®
Bioorganic & Medicinal Chemistry 14 (2006) 1189–1198
Bioorganic & Medicinal Chemistry

Induction of apoptosis in HeLa cells by 3β-hydroxy-12-oleanen-27-oic acid from the rhizomes of *Astilbe chinensis*

Hong-Xiang Sun,* Quan-Fang Zheng and Jue Tu

College of Animal Sciences, Zhejiang University, Hangzhou 310029, China

Received 19 August 2005; revised 16 September 2005; accepted 16 September 2005
Available online 7 October 2005

Abstract—3β-Hydroxy-12-oleanen-27-oic acid (ATA) was an antitumor active oleanane-type triterpenoid from the rhizomes of *Astilbe chinensis*. ATA was structurally very similar to oleanolic acid, with the only difference being interchange of the carboxyl and methyl groups at the C-14 and C-17 positions. Oleanane-type triterpene with a carboxyl group at C-14 is present in a limited number of natural resources. ATA was found to exhibit more distinctive cytotoxicity toward human cervical squamous carcinoma HeLa cells than oleanolic acid, which suggested that the position of the carboxyl group significantly affects the cytotoxicity of oleanane-type pentacyclic triterpenes with a carboxyl group. The biological mechanism responsible for the cytotoxicity of ATA is not yet well understood. In this study, we investigated the induction of apoptosis in HeLa cells by ATA and the putative pathways of its actions. ATA induced a marked concentration- and time-dependent inhibition of HeLa cell proliferation, and reduced the protein content in HeLa cells. ATA-treated HeLa displayed typical morphological apoptotic characteristics and formation of DNA ladders in agarose gel electrophoresis. Flow cytometric analysis showed that the HeLa cell cycle was arrested in the G_0/G_1 phase by ATA, and the apoptotic rate of HeLa cells treated with ATA 20 μg/mL for 48 h was 22.63 ± 1.65%. Meanwhile, ATA increased the expression of Bax, decreased the expression of Bcl-2, and lowered the $\Delta\Psi_m$. DEVD-CHO 2 μM could increase the viability of ATA-treated HeLa cells. These results indicate that ATA could significantly induce cell apoptosis through down-regulating Bcl-2 expression, up-regulating Bax expression, lowering $\Delta\Psi_m$, and activating the caspase-3 pathway, and should be useful in the search for new potential anti-tumor agents and for developing semisynthetic oleanane-type triterpene derivatives with anti-tumor activity.

1. Introduction

Natural products have been shown to be excellent and reliable source for the development of new drugs.[1] Many natural products have pharmacological applications, in particular their potential for use in cancer chemoprevention.[2,3] Indeed, amongst the well-known anti-cancer drugs are the well-known *Cantharanthus* alkaloids, colchicine, etoposide, and taxol.[4,5]

Triterpenes represent a varied class of natural products. Thousands of structures have been reported with hundreds of new derivatives described each year.[6] Triterpenes are the major constituents of some medicinal herbs and are widely present in all parts of a variety of plants. Recently, several triterpenes have been described to induce apoptosis in different cell types.[7,8] Among these compounds, pentacyclic triterpenes such as amooranin,[9] asiatic acid,[10] *epi*-oleanolic acid,[11] oleanolic acid,[12,13] and ursolic acid,[14,15] for example, have been found to inhibit tumor cell proliferation and tumor growth, and induce differentiation and apoptosis.

We have earlier reported the isolation and structure elucidation of three cytotoxic pentacyclic triterpenoids, 3β-hydroxy-12-oleanen-27-oic acid (ATA) (Fig. 1), 3β, 6β-dihydroxy-12-oleanen-27-oic acid (ATB), and 3β-acetyl-12-oleanen-27-oic acid (ATC), from the rhizomes of *Astilbe chinensis* (Maxim.) Franch. et Savat. (Saxifragaceae).[16] The structures of ATA and ATB were confirmed by a single crystal X-ray diffraction analysis.[17,18] We have also reported the cytotoxic activity of these compounds toward human ovarian carcinoma HO-8910 cells, human cervical squamous carcinoma HeLa cells, and human leukemic HL60 cells.[19] These compounds all belong to 12-oleanen-27-oic acid derivatives. Among

Keywords: 3β-Hydroxy-12-oleanen-27-oic acid; HeLa cells; Apoptosis; Cell cycle; Bcl-2; Bax; Mitochondrial transmembrane potential ($\Delta\Psi_m$); Caspase-3.
* Corresponding author. Tel.: +86 571 8697 1091; fax: +86 571 8697 1316; e-mail: sunhx@zju.edu.cn

0968-0896/$ - see front matter © 2005 Elsevier Ltd. All rights reserved.
doi:10.1016/j.bmc.2005.09.043

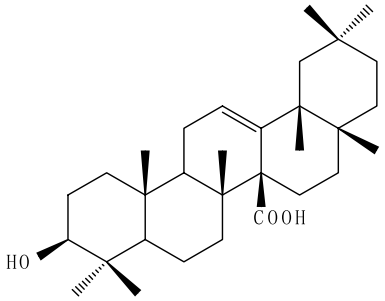

Figure 1. Structure of 3β-hydroxy-12-oleanen-27-oic acid (ATA, $C_{30}H_{48}O_3$, HREI-MS: 456.3594).

three triterpenes, the order of the cytotoxic activity in terms of the IC_{50} values against the above three tumor cell lines was ATA > ATC > ATB. Oleananes constitute what is probably the largest and most important group of triterpenes. ATA was structurally very similar to oleanolic acid, with the only difference being interchange of the carboxyl and methyl groups at the C-14 and C-17 positions. Oleanolic acid gives its name to the wider group and is a compound fairly abundant in plants, whereas the 27-carboxyl homologue is present in a limited number of natural resources. Moreover, the biological mechanism responsible for the cytotoxicity of ATA is not yet well understood. Thus, in this study we investigated the effects on induction of apoptosis in HeLa cells and the putative pathways of actions of ATA.

2. Results

2.1. Growth inhibitory effect of ATA on HeLa cells

Growth inhibitory effects of ATA on HeLa cells were determined by 3-(4,5-dimethylthiazol-2-yl)-2,5-diphenyl tetrazolium bromide (MTT) method. ATA significantly inhibited the growth of HeLa cells in a concentration-dependent manner. The IC_{50} of ATA against HeLa cell was approximately 6.49 ± 0.33 μg/mL following a 48 h incubation, while the IC_{50} of CDDP was 2.07 ± 0.19 μg/mL determined under the same condition. As shown in Figure 2, ATA induced a marked concentration- and time-dependent inhibition of HeLa cell proliferation by a growth curve. Determination of protein content showed that ATA significantly reduced the total protein content in HeLa cells in a dose-dependent manner (Fig. 3).

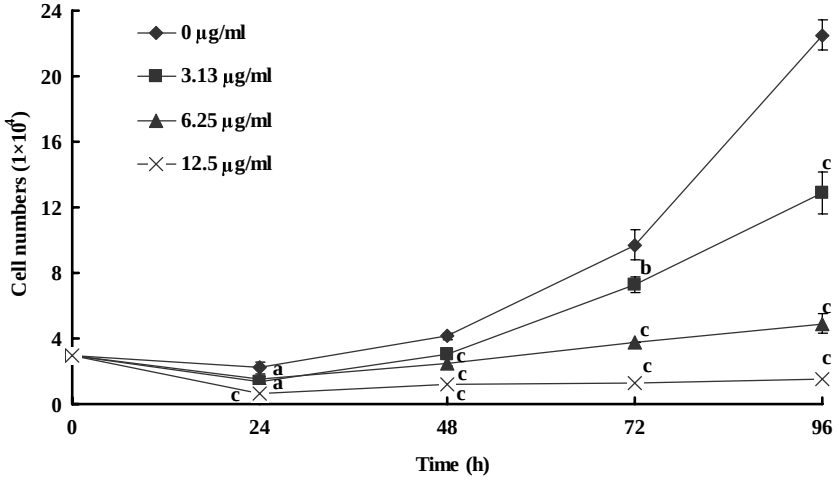

Figure 2. Effect of ATA on HeLa cell growth. The values are presented as means ± SE ($n = 4$). Significant differences with 0 μg/mL were designated as $^{a}P < 0.05$, $^{b}P < 0.01$, and $^{c}P < 0.001$.

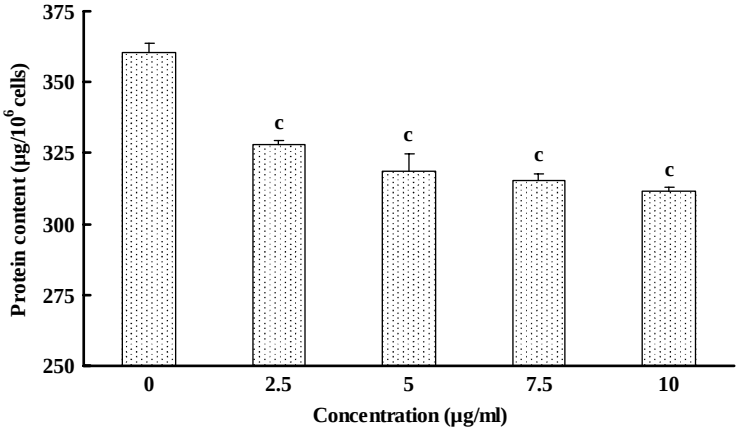

Figure 3. Effect of ATA on protein contents in HeLa cells. The values are presented as means ± SE ($n = 6$). Significant differences with 0 μg/mL were designated as $^{c}P < 0.001$.

2.2. Effect of ATA on morphology of HeLa cells

ATA-treated cells stained with Giemsa showed clear apoptotic characteristics, such as condensation of nuclear, nuclear fragmentation, membrane blebbing, and apoptotic bodies (Figs. 4B–D). Under a fluorescence microscope, the DNA in the nucleus of control cells showed homogeneously Kelly fluorescence, while ATA-treated cells showed typical apoptotic features characterized by volume reduction, chromatin condensation, nuclear fragmentation with dense Kelly fluorescence stain, and appearance of apoptotic bodies (Figs. 5B and C). Electron microscope observation revealed that numerous ATA-treated cells showed that volume

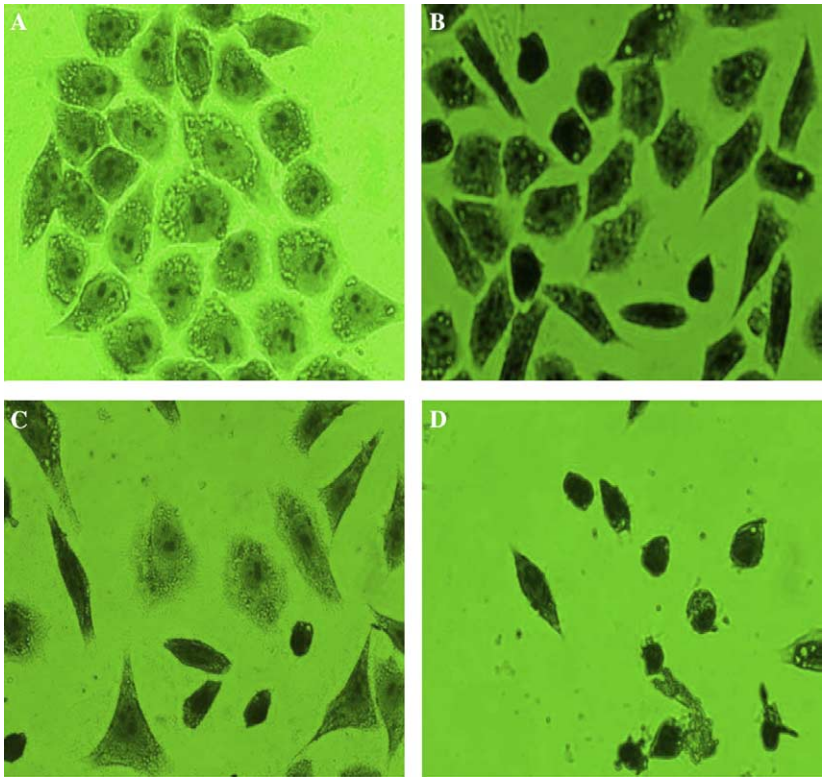

Figure 4. Morphological changes of ATA-treated HeLa cells stained with Giemsa microscopy (magnification, 400×). (A) Cell control; (B) 7.5 μg/mL; (C) 10 μg/mL; and (D) 15 μg/mL. The figures shown are representative of three independent experiments.

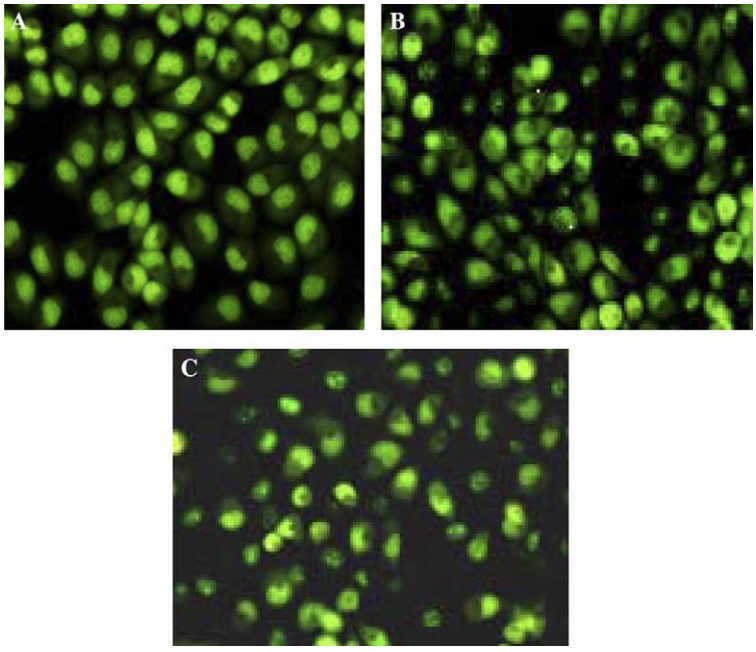

Figure 5. Morphological changes of ATA-treated HeLa cells stained with acridine orange. (A) Cell control; (B) 10 μg/mL; (C) 15 μg/mL. The figures shown are representative of three independent experiments.

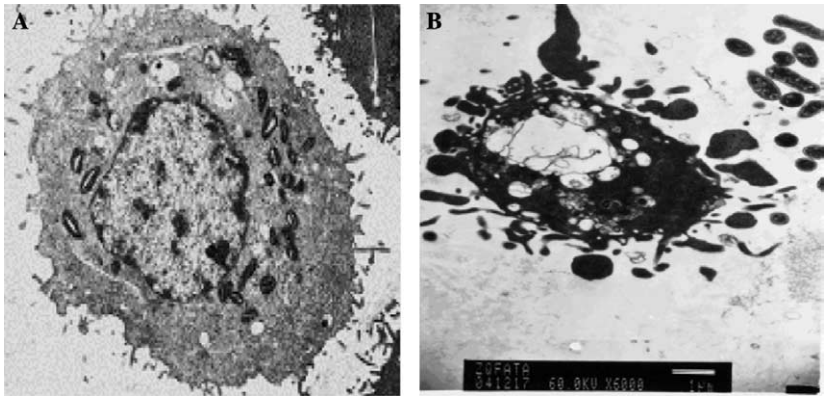

Figure 6. Characteristic morphology of ATA-induced apoptosis of HeLa cells by an electron microscopy. (A) Cell control (magnification, 4000×); (B) 15 μg/mL (magnification, 6000×).

reduced, cytoplasm shrunk, plasma membrane remained well defined, chromatin condensed, and located along nuclear envelope or formed irregularly shaped crescents at nuclear edges (Fig. 6B) as compared with untreated cells (Fig. 6A).

2.3. Effects of ATA on DNA fragmentation of HeLa cells

DNA isolated from HeLa cells cultured with ATA 15 and 20 μg/mL for 24 h showed a characteristic 'ladder' pattern of apoptosis. A comparison with molecular weight markers indicated that the fragments were multiples of approximately 180 bp (Fig. 7).

2.4. Effect of ATA on apoptosis rate and cell cycle distribution of HeLa cells

After treatment of HeLa cells with different concentrations (5, 10, and 15 μg/mL) of ATA for 24 h, the obvious changes in cell cycle distribution of the ATA-treated cells were characterized by increase of G_0/G_1 phase and decrease of S and G_2/M phase cells in a dose-dependent manner, suggesting that ATA could suppress HeLa cell proliferation associated with cell cycle arrest in G_0/G_1 phase (Fig. 8). After treatment of HeLa cells with ATA

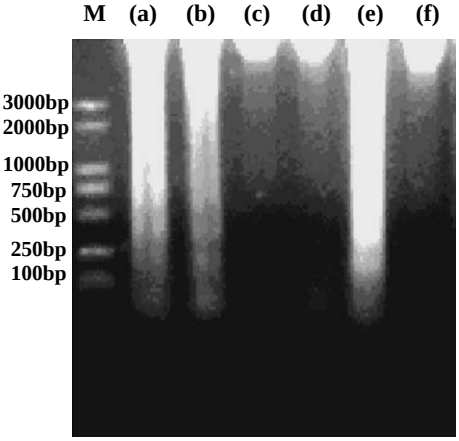

Figure 7. Agarose gel electrophoresis for detecting DNA fragmentation in HeLa cells treated with ATA for 24 h. Lane a, ATA 20 μg/mL; lane b, ATA 15 μg/mL; lane c, ATA 10 μg/mL; lane d, ATA 7.5 μg/mL; lane e, CDDP 8 μg/mL; lane f, cell control; lane M, DNA marker.

15 and 20 μg/mL for 24 h, a subdiploid peak of DNA characteristic of apoptotic was observed, and the apoptosis rate was 8.08 ± 1.63% ($P < 0.01$) and 22.63 ± 1.65% ($P < 0.001$) for 15 and 20 μg/mL, respectively (Fig. 9).

2.5. Effect of ATA on expression of Bcl-2 and Bax proteins in HeLa cells

Bcl-2 has been reported to inhibit apoptosis, while Bax has been reported to enhance apoptosis. To examine the role of these Bcl-2 family genes in ATA-induced apoptosis, the expressions of Bcl-2 and Bax proteins were evaluated in HeLa cells using a SABC immunohistochemical method. As shown in Table 1, compared to control cells, Bel-2 protein expression was markedly decreased and Bax protein expression was highly increased in ATA-treated HeLa cells, suggesting ATA down-regulated Bcl-2 protein level and up-regulated Bax protein level.

2.6. Effect of ATA on $\Delta\Psi_m$ in HeLa cells

$\Delta\Psi_m$ collapse is a critical step that occurs in all cell types undergoing apoptosis, regardless of the inductive signal. To assess the effect of ATA on the $\Delta\Psi_m$ and to determine whether cells with a low $\Delta\Psi_m$ also lose plasma membrane integrity, we double stained ATA-treated and control HeLa cells with PI and Rh123, a lipophilic cation that is taken up by mitochondria in proportion to the $\Delta\Psi_m$. As shown in Figure 10A, control living cells were PI negative and strongly stained by Rh123 (PI^-Rh123^+, homeostasis, $\Delta\Psi_m$ high). With ATA treatment, a fraction of Pi-negative and low-Rh123-staining (PI^-Rh123, apoptosis, $\Delta\Psi_m$ low) HeLa cells appeared significantly ($P < 0.05$) in a dose-dependent manner (Table 2 and Figs. 10B–F). However, no significant differences ($P > 0.05$) were observed in cell death (PI^+Rh123^-) between control and ATA-treated cells. These results suggest that ATA decreased the $\Delta\Psi_m$ without altering plasma membrane permeability in HeLa cells.

2.7. Effect of DEVD-CHO on viability of ATA-treated HeLa cells

Caspase-3 plays a critical role in apoptosis and caspase-3 activity has been suggested as an index of

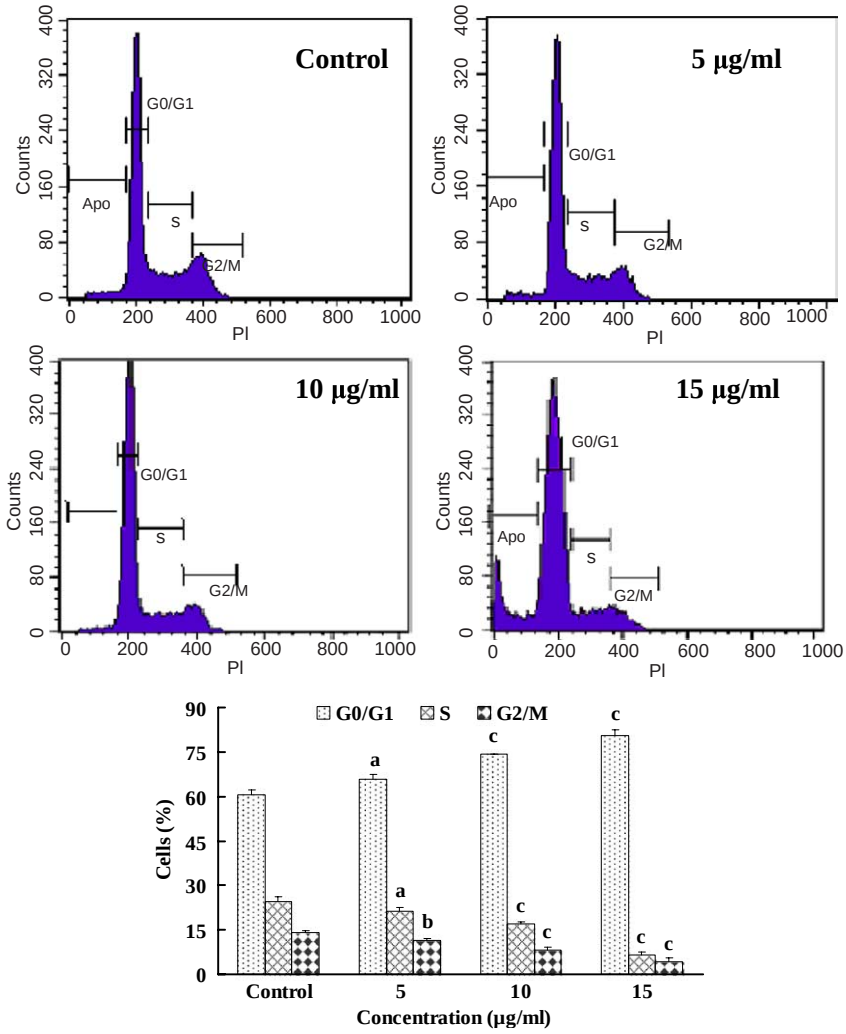

Figure 8. Effect of ATA on cell cycle distribution in HeLa cells. The histogram demonstrates the percentage of cells in various phases in HeLa cells treated with ATA. The values are presented as means ± SE ($n = 5$). Significant differences with 0 μg/mL were designated $^{a}P < 0.05$, $^{b}P < 0.01$, and $^{c}P < 0.001$.

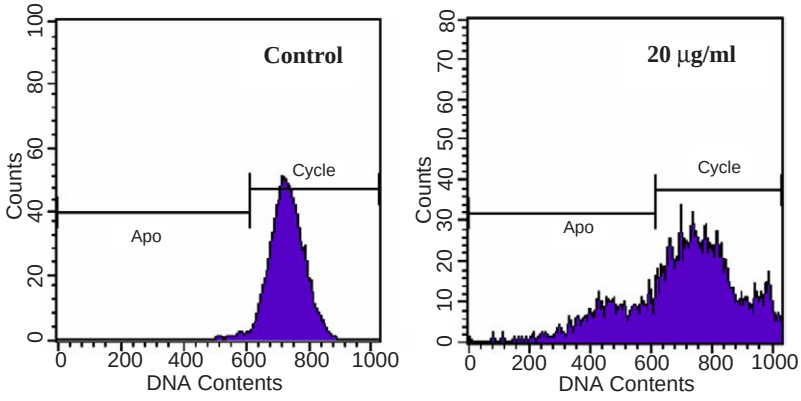

Figure 9. Effect of ATA on apoptotic rate in HeLa cells. After treatment without or with 20 μg/mL ATA, cells were stained with propidium iodide (PI), with apoptotic rate measured by flow cytometry.

apoptosis. After incubation with cell-permeable DEVD-CHO 2 μM or RPMI 1640 for 1 h, HeLa cells were administered with different concentrations of ATA, respectively, and the viability was measured by the MTT assay 48 h later. As shown in Figure 11, DEVD-CHO 2 μM could significantly increase the viability of HeLa cell treated with ATA (⩽10 μg/mL) for 48 h.

Table 1. Effect of ATA on the expression of Bcl-2 and Bax proteins of HeLa cells after 48 h treatment

Concentration (μg/mL)	Bcl-2 (%)	Bax (%)	Bcl-2/Bax value
Control	45.7 ± 5.18	21.05 ± 4.41	2.17
5	37.25 ± 5.55[a]	27.54 ± 1.44	1.35
7.5	26.05 ± 3.35[b]	35.53 ± 5.32[c]	0.73
10	19.64 ± 1.32[c]	40.08 ± 2.83[c]	0.49

The values are expressed as means ± SE ($n = 5$). Significant differences with control cells were designated as [a]$P < 0.05$, [b]$P < 0.01$, and [c]$P < 0.001$.

Table 2. Change of $\Delta\Psi_m$ in HeLa cells treated with ATA for 24 h

Concentration (μg/mL)	PI^-Rh123^-	PI^-Rh123^+	PI^+Rh123^-
Control	1.18 ± 0.27	97.55 ± 0.24	1.29 ± 0.42
5	4.42 ± 0.95[a]	96.12 ± 0.89[a]	0.75 ± 0.16
10	4.47 ± 0.24[a]	94.58 ± 1.21[b]	0.64 ± 0.49
15	9.62 ± 2.60[b]	89.58 ± 2.56[b]	0.78 ± 0.02
20	19.60 ± 1.69[c]	79.02 ± 1.75[c]	1.10 ± 0.15

The values are expressed as mean ± SE ($n = 5$). Significant differences with control cells were designated as [a]$P < 0.05$, [b]$P < 0.01$, and [c]$P < 0.001$.

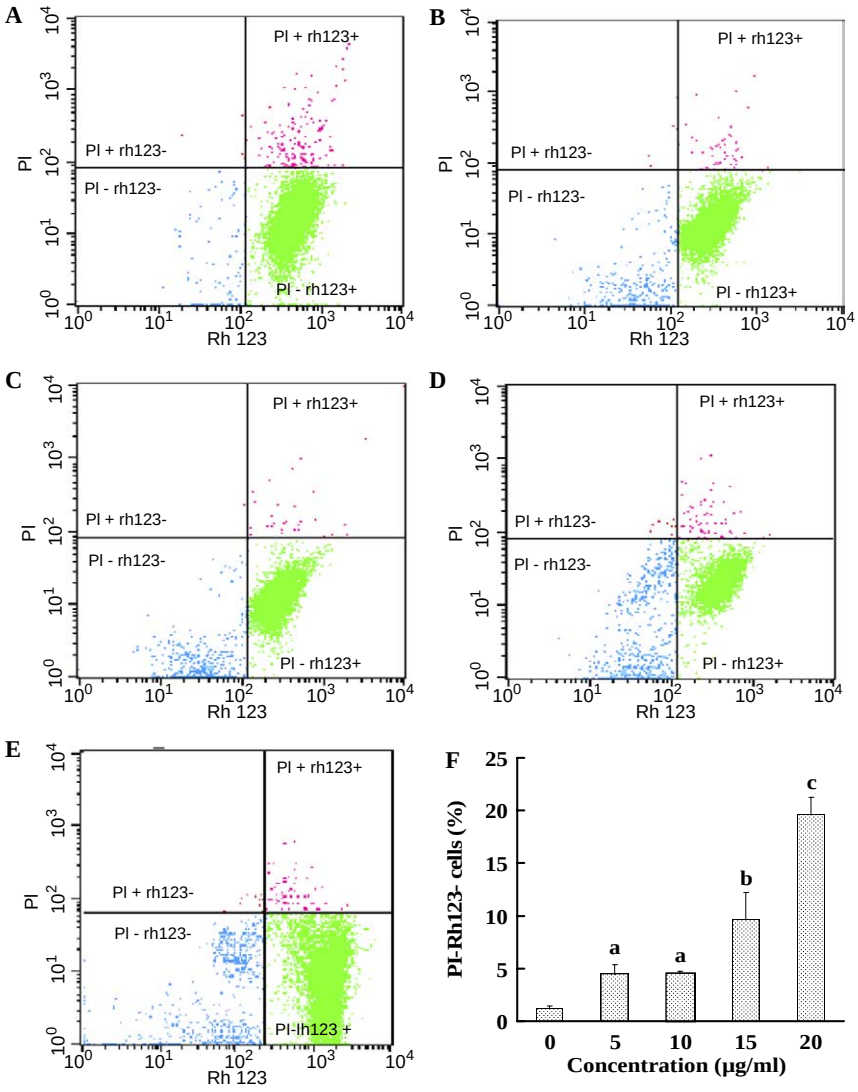

Figure 10. Effects of ATA on the mitochondrial transmembrane potential ($\Delta\Psi_m$) in HeLa cells. (A–E) scatter plots of HeLa cells cultured with ATA 0, 5, 10, 15, and 20 μg/mL, respectively. The histogram demonstrates the percentage of PI^-Rh123^- cells in HeLa cells treated with ATA. The values are presented as means ± SE ($n = 5$). Significant differences with 0 μg/mL were designated as [a]$P < 0.05$, [b]$P < 0.01$, and [c]$P < 0.001$.

3. Discussion

ATA from the rhizomes of *A. chinensis* was an oleanane-type pentacyclic triterpene with a carboxyl group at C-14. In the past few years, a number of pentacyclic triterpenoids with potent anti-cancer activity were reported.[7,8] Oleananes constitute what is probably the largest and most important group of pentacyclic triterpenes. Oleanolic acid gives its name to the wider group and is a compound fairly abundant in plants, whereas, to our knowledge, the oleanane-type triterpenoid showing the presence of a carboxyl group at C-14 position is present in a limited number of natural resources. The cytotoxic effect against HO-8910, HeLa and HL60, and apoptosis-inducing effect on the HO-8910 cells by ATA were reported.[19] However, its further mechanisms underlying the antitumor activity were unclear.

Inhibition of cancer growth has been a continuous effort in cancer treatment. A reduction in cell growth and an

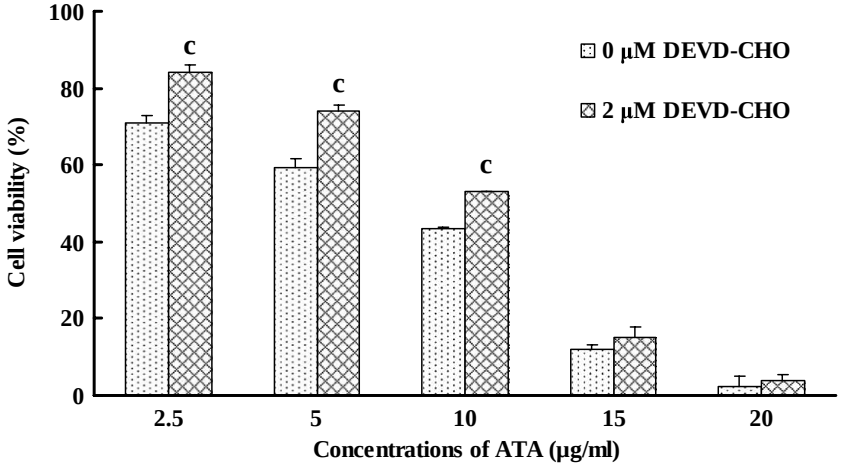

Figure 11. Effect of DEVD-CHO on the viability of HeLa cells treated with ATA. The values are presented as means ± SE ($n = 5$). Significant differences with 0 μM were designated as $^{c}P < 0.001$.

induction in cell death are two major means to inhibit tumor growth.[20] In this study, we demonstrated that ATA induced a marked concentration- and time-dependent inhibition of HeLa cell proliferation with an IC_{50} of 6.49 ± 0.33 μg/mL following 48 h incubation and reduced the protein content in HeLa cell. However, the IC_{50} of oleanolic acid was greater than 100 μg/mL determined under the same condition. It implicated a higher cytotoxic activity for ATA than that for oleanolic acid. The results suggested that the position of carboxyl group significantly affects the cytotoxicity of oleanane-type pentacyclic triterpenes with a carboxyl group. We have compared the cytotoxic activity of ATA, ATB, and ATC toward HO-8910, HeLa, and HL60 cells, and found that the order of the cytotoxic activity in terms of the IC_{50} values against the above three tumor cell lines was ATA > ATC > ATB. The stucture of ATB differs from the structure of ATA by the addition of a β-hydroxy at position C-6 and ATC is the 3β-acetylate of ATA. In addition, we have converted ATA into 3-disodiumphosphate and determined its IC_{50} values toward HO-8910, HeLa, and HL60 cells. The IC_{50} values of ATA 3-disodiumphosphate against these tumor cells were also greater than 100 μg/mL. These results indicate that specific differences in chemical structure of the oleanane-type triterpene with a carboxyl group at C-14 will influence the cytotoxic properties and proliferation of tumor cells, and 3β-OH has a crucial affect on their antitumor action.

Apoptosis, also known as programmed cell death, is characterized by distinct morphological features such as cell shrinkage, chromatin condensation, plasma membrane blebbing, oligonucleosomal DNA fragmentation, and finally the break down of the cell into smaller units (apoptotic bodies).[21] To determine ATA-induced apoptosis in cancer cells, nuclear morphology in HeLa cells was analyzed using Giemsa staining, acridine orange fluorescent staining, and the transmission electron microscope. The morphologic observations revealed apoptotic changes including apoptotic morphology of cellular bodies and the chromatin condensation (Figs. 4–6). In addition, it is known that DNA strand breaks occur during the process of apoptosis, and the DNA fragmentation in HeLa cells was detected using agarose gel electrophoresis. The results indicated that ATA could cause HeLa cells, oligonucleosomal DNA fragmentation (Fig. 7). Apoptosis induced by anticancer drugs is a concentration–time limited course of cell death associated with several morphological and biochemical events, eventually resulting in secondary necrosis, and it was confirmed in our experiments. According to the results of flow cytometric analysis, ATA could suppress HeLa cell proliferation associated with cell cycle arrest in the G_0/G_1 phase (Figs. 8A–E). The ratio of apoptotic cells detected by a flow cytometer was 8.08 ± 1.63% ($P < 0.01$) and 22.63 ± 1.65% for 15 and 20 μg/mL, respectively (Fig. 9). Thus, ATA possessed antitumor activity through inducing cell apoptosis.[22]

It has been documented that the progress of apoptosis is regulated by the expression of several transcriptional genes. One of these genes is a member of the Bcl-2 family.[23] The proapoptotic and antiapoptotic members of the Bcl-2 family act as a rheostat in regulating programmed cell death and as a target of anticancer therapy. The Bcl-2 family can be classified into two functionally distinct groups: anti-apoptotic genes and pro-apoptotic genes. Bcl-2, an anti-apoptotic gene, is known for regulating the apoptotic pathways and protecting cell death, while Bax, a pro-apoptotic gene of the family, is expressed abundantly and selectively during apoptosis, promoting cell death.[24] The Bcl-2 protein encoded by the Bcl-2 proto-oncogene, predominantly localized on the outer mitochondrial membrane, plays a central role in the regulation of cell proliferation and apoptosis. Bax, a related homologue of the Bcl-2 protein predominantly localized in the cytosol, forms heterodimers with Bcl-2, effectively antagonizing Bcl-2 function and thus promoting apoptosis. In addition, Bax dimers or oligomers directly form a channel in the mitochondrial outer membrane, translocate to the mitochondria, and trigger the loss of $\Delta\Psi_m$, mediating the release of cytochrome *c* in apoptosis.[25] Bax/Bcl-2 ratio in a cell acts to regulate its own susceptibility to apoptosis.[26] In the present study, we demonstrated that the expression of Bcl-2 was decreased, while that of Bax was increased,

and the ratio of Bcl-2 and Bax was reduced significantly (Table 1), which correlated well with ATA-induced apoptosis in HeLa cells.

Recently, $\Delta\Psi_m$ collapse has been shown to play an essential role in mediating apoptosis in that it allows the release into cytoplasm of apoptotic mediators, such as cytochrome *c* and apoptosis-inducing factor. In turn, cytochrome *c* and the apoptosis-inducing factor directly or indirectly activate members of the caspase family, which are regarded as death effector molecules.[27] As the downstream event of the high Bax/Bcl-2 ratio, we examined the mitochondria transition potential ($\Delta\Psi_m$), which was the evidence for mitochondria membrane permeability. Our experiment showed that the $\Delta\Psi_m$ in HeLa cells treated with ATA was decreased significantly (Table 2 and Fig. 10), which was an evidence for the alterations of permeability of outer membrane of mitochondria. The lowered level of $\Delta\Psi_m$ is the upstream event of caspase activation, which will finally lead the cell to apoptosis at last.

At the execution phase of apoptosis, a series of morphological and biochemical changes appear to have resulted from the action of cysteine-dependent aspartate-directed proteases, caspases.[26] Caspase-3, in particular, is believed to be one of the most commonly involved mechanisms in the execution of apoptosis in various cell types.[28] We examined the effect of DEVD-CHO, a highly specific and potent inhibitor of caspase-3, on the inhibition of ATA-treated HeLa cell proliferation and found that DEVD-CHO blocked ATA-induced inhibition (Fig. 11). It suggested that the activation of caspase-3 was necessary for the execution of apoptosis induced by ATA.

Since ATA is able to significantly inhibit HeLa cell proliferation and induce cell apoptosis through down-regulating Bcl-2 expression, up-regulating Bax expression, lowering $\Delta\Psi_m$, and activating the caspase-3 pathway, these results should be useful in the search for new potential anti-tumor agents and for developing semisynthetic oleanane-type triterpene derivatives with anti-tumor activity.

4. Experimental

4.1. Drugs

3β-Hydroxy-12-oleanen-27-oic acid (ATA) was previously isolated by us from the rhizomes of *A. chinensis* (Saxifragaceae).[16] The structure of ATA was elucidated by spectroscopic analysis including two-dimensional NMR spectroscopy and confirmed by single-crystal X-ray diffraction analysis.[17] The positive drug, *cis*-diamminedichloride platinum (CDDP), was obtained from Sigma Chemical Co. (St. Louis, MO, USA).

4.2. Cell culture

Human cervical squamous carcinoma (HeLa) cells were maintained in the logarithmic phase of growth in RPMI 1640 medium (Gibco-BRL, Grand Island, NY) supplemented with 10% fetal bovine serum (Gibco-BRL), 2 mM L-glutamine (Sigma Chemical Co., St. Louis, MO) at 37 °C under humidified air with 5% CO_2.

4.3. Cell proliferation and viability assay

The 50% inhibitory concentration (IC_{50}) of ATA on HeLa cells was determined by the MTT assay. Briefly, HeLa cells were seeded at 1×10^4 cells/well in a 96-well plate (Nunc) and incubated at 37 °C in a humidified atmosphere with 5% CO_2. After 24 h, the various concentrations of ATA were added into each well and these cells were incubated at 37 °C. Each concentration was repeated in four wells. After 48 h, 50 μl MTT solutions (2 mg/mL) were added to each well and incubated at 37 °C for further 2 h. The medium was removed, and 150 μl of DMSO working solution was added to each well. The OD was measured at 570 nm by an ELISA reader (Shanghai, China). The inhibited rate and IC_{50} of ATA on HeLa cell proliferation were calculated by the NDST software. Each test was performed in triplicate.

The effect of ATA on the growth curve of HeLa cells was determined according to the methods. Briefly, HeLa cells were seeded at 3×10^4 cells/well in 24-well plate (Nunc), and then various ATA concentrations (final drug concentration 0, 3.125, 6.25, and 12.5 μg/mL) were directly added to each well. The plates were incubated at 37 °C in a 5% CO_2 humidified atmosphere for 0, 12, 24, 36, 48, and 60 h, respectively. The number of cultured cells was counted with a hemocytometer following staining with 0.4% trypan blue.

4.4. Determination of protein content

The protein contents in HeLa cells treated with ATA 0, 2.5, 5, 7.5, and 10 μg/mL for 48 h were measured by the Coomassie dye binding method. Briefly, 1×10^6 cells for each concentration were harvested and washed by PBS, and then the cell pellets were reacted with 1 ml of 1% sodium dodecyl sulfate (SDS, Shanghai Shenergy Biocolor Co., Shanghai, China) for 30 min at 100 °C. The lysed solution was treated with Coomassie dye G-250 (Bioasia, Palo Alto, CA, USA) solution (0.1 mg/mL) at room temperature for 10 min, and then the absorbance of the solution was measured at 595 nm with UV-754 ultra-violet spectrophotometer (Shanghai Third Analysis Instrument Factory). The calibration curves were constructed with standard samples bovine serum albumin (BSA, Bovogen, Victoria, Australia) in triplicate and consisted of six standard samples. The calibration curves were linear over the range of 1–50 μg/mL for BSA, with $r = 0.9994$.

4.5. Morphological analysis

Giemsa-staining microscopic observation was performed as follows. Briefly, HeLa cells were seeded at 1×10^5 cells/well in a six-well plate (Nunc). The plates were then incubated at 37 °C in a humid atmosphere with 5% CO_2. After 24 h, ATA of various concentrations was added to the

cultures, and the plates were then incubated for further 24 h. Cultured cells were stained with *Giemsa* solution for 15–30 min and then visualized by an Olympus microscope.

The fluorescence microscope observation was performed according to the methods. Briefly, HeLa cells (1×10^5 cells/ml) were seeded into a 24-well plate (Nunc). The plates were then incubated at 37 °C in a humid atmosphere with 5% CO_2. ATA of various concentrations was added to the cultures 24 h after subculture. After 24 h, the 24-well plate cells were taken out, and HeLa cells were stained with 100 μl acridine orange (AO, Amersco, Ohio, USA) solution (5 μg/mL) and then visualized by fluorescence microscope.

The transmission electron microscope observation was performed according to the methods. Briefly, after a 24 h exposure to ATA 0 and 15 μg/mL, HeLa cells were fixed with 2.5% glutaraldehyde and 1% osmiumtetraoxide. After dehydration, the samples were embedded in Epo812 and then ultramicrotomed. The sections were routinely stained and examined by a JEM-1230 electron microscope (JEOL, Japan).

4.6. DNA fragmentation analysis

After incubation with ATA 0, 7.5, 10, 15, and 20 μg/mL for 24 h, DNA fragmentation was analyzed by electrophoresis as previously described. Briefly, after trypsinization, cells (1.0×10^7 cells per sample) were washed with TBS (pH 7.6) and collected by centrifugation at 1000*g* for 10 min. The pellet was resuspended in 500 μl lysis solution (10 mmol/L Tris–HCl (pH 8.0), 150 mmol/L NaCl, 10 mmol/L EDTA, 0.4% SDS, and 100 μg/mL proteinase K) for 2 h at 50 °C. The sample was then extracted with equal volumes of phenol/chloroform/isoamyl alcohol (25:24:1) (Shanghai Shenergy Biocology, Shanghai, China). DNA was precipitated by ethanol, air-dried, and dissolved in TE buffer (Tris–HCl 5 mmol/L (pH 8.0) and edetic acid 20 mmol/L) containing ribonuclease A (RNase A) 0.1 mg/mL. The samples were run on 1.5% agarose gels containing ethidium bromide 0.5 g/L and visualized under UV illumination.

4.7. Flow cytometric analysis

After exposure to ATA 0, 5, 10, 15, and 20 μg/mL for 24 h, cultured HeLa cells were collected and fixed with 70% ethanol. Quantitative detection of apoptotic cells and analysis of cell cycle distribution in cultures were performed by a FACScan flow cytometer using the CellQuest 3.0f software (Becton–Dickinson, Franklin Lakes, NJ), and the data were analyzed on Modfit 3.0 DNA software. Each test was performed five times.

4.8. SABC immunohistochemical analysis

After a 24-h exposure to ATA 0, 5, 7.5, and 10 μg/mL, the expressions of Bel-2 and Bax proteins in HeLa cells were visualized by immunohistochemical assay kit according to the manufacturer's specifications (Wuhan Boster Biological Technology Ltd., Wuhan, China).[29] Briefly, cultured cell sections were fixed with 4% paraformaldehyde and endogenous peroxidase activity was blocked with H_2O_2 and normal goat serum. Then, the sections were incubated with the rabbit anti-human Bcl-2 or Bax polyclonal antibody, respectively, biotinylated goat antirabbit IgG, and avidin–biotin–peroxidase complex in turn. After being stained by DAB, the sections were observed under a light microscope. Photographs were taken and a quantitative analysis was conducted with td2000 pathology cell image analysis system in 5 areas of each slide.

4.9. Measurement of mitochondrial transmembrane potential ($\Delta\Psi_m$)

After treatment with ATA 0, 5, 10, 15, and 20 μg/mL for 24 h, the changes of $\Delta\Psi_m$) in cultured cells were analyzed using a FACScan flow cytometer.[30] Briefly, after trypsinization, cells were washed twice with PBS, and then the concentration of cell suspension was adjusted to 1×10^6 cells/ml. One hundred microliter rhodamine 123 (Rh123) solution (20 μg/mL) was added to 100 μl of cell suspension. After incubation at 37 °C for 30 min, the cells were washed with PBS again and stained with propidium iodide (PI) solution (100 μg/mL). The Rh123 and PI staining fluorescence of individual cell was measured with FCM. All data were collected, stored, and analyzed with the use of Cellquest 3.1f Analysis Software.

4.10. Detection of viability of HeLa cells treated with ATA or DEVD-CHO and ATA

As caspase-3 activation is a key step in the regulation of apoptosis. Viability of HeLa cells treated with caspase-3 inhibitor DEVD-CHO (Asp-Glu-Val-Asp-Aldehyde, Biomol, Plymouth Meeting, PA, USA) and ATA was measured by the MTT assay.[31,32] After an incubation with DEVD-CHO 2 μmol/L or RPMI 1640 for 1 h, HeLa cells were administered with ATA (final concentration 0, 2.5, 5, 10, 15, and 20 μg/mL), and the viability was measured by the MTT assay 48 h later.

Acknowledgments

This work was supported by Grants-in-Aid from the Zhejiang Provincial Natural Science Foundation of China (No. 300456, Y204095), the Zhejiang Provincial Science and Technology Council (No. 2002C3306), and the Administration of Traditional Chinese Medicine of Zhejiang Province (No. 2002KF02).

References and notes

1. Newman, D. J.; Cragg, G. M.; Snader, K. M. *Nat. Prod. Rep.* **2000**, *17*, 215.
2. Graham, J. G.; Quinn, D. M. L.; Fabricant, S.; Farnsworth, N. R. *J. Ethnopharmacol.* **2000**, *73*, 347.
3. Kamuhabwa, A.; Nshimo, C.; Witte, P. *J. Ethnopharmacol.* **2000**, *70*, 143.
4. Calabrese, R.; Chabner, B. A. In *The Pharmacological Basis of Therapeutics*; Gilman, A. G., Goodman, L. S.,

Gilman, J. W., Eds.; MacGraw Hill: New York, pp 1225–1287.
5. Pezzuto, J. M. *Biochem. Pharmacol.* **1997**, *53*, 121.
6. Connolly, J. D.; Hill, R. A. *Nat. Prod. Rep.* **2005**, *22*, 487.
7. Ovesna, Z.; Vachalkova, A.; Horvathova, K.; Tothova, D. *Neoplasma* **2004**, *51*, 327.
8. Chiang, L. C.; Chiang, W.; Chang, M. Y.; Ng, L. T.; Lin, C. C. *Am. J. Chin. Med.* **2003**, *31*, 37.
9. Rabi, T.; Ramachandran, C.; Fonseca, H. B.; Nair, R. P.; Alamo, A.; Melnick, S. J.; Escalon, E. *Breast Cancer Res. Treat.* **2003**, *80*, 321.
10. Park, B. C.; Bosire, K. O.; Lee, E. S.; Lee, Y. S.; Kim, J. A. *Cancer Lett.* **2005**, *218*, 81.
11. Jung, M. J.; Yoo, Y. C.; Lee, K. B.; Kim, J. B.; Song, K. S. *Arch. Pharm. Res.* **2004**, *27*, 840.
12. Fernandes, J.; Castilho, R. O.; da Costa, M. R.; Wagner-Souza, K.; Coelho Kaplan, M. A.; Gattass, C. R. *Cancer Lett.* **2003**, *190*, 165.
13. Hsu, H. Y.; Yang, J. J.; Lin, C. C. *Cancer Lett.* **1997**, *111*, 7.
14. Hsu, Y. L.; Kuo, P. L.; Lin, C. C. *Life Sci.* **2004**, *75*, 2303.
15. Shishodia, S.; Majumdar, S.; Banerjee, S.; Aggarwal, B. B. *Cancer Res.* **2003**, *63*, 4375.
16. Sun, H. X.; Zhang, J. X.; Ye, Y. P.; Pan, Y. J.; Shen, Y. M. *Helv. Chim. Acta* **2003**, *86*, 2414.
17. Sun, H. X.; Ye, Y. P.; Wang, K. W.; Pan, Y. J. *Acta Crystallogr. E* **2003**, *59*, 0989.
18. Sun, H. X.; Pan, Y. J. *Acta Crystallogr. C* **2004**, *60*, O300.
19. Sun, H. X.; Ye, Y. P.; Pan, Y. J. *J. Ethnopharmacol* **2004**, *90*, 261.
20. Hyun, P. W.; Hee, C. Y.; Won, J. C.; Oh, P. J.; Kim, K.; Hyuck, I. Y.; Lee, M. H.; Ki, K. W.; Park, K. *Biochem. Biophys. Res. Commun.* **2003**, *300*, 230.
21. Earnshaw, W. C. *Curr. Opin. Cell Biol.* **1995**, *7*, 337.
22. Evan, G.; Littlewood, T. *Science* **1998**, *281*, 1317.
23. Korsmeyer, S. J. *Cancer Res.* **1999**, *59*, 1693.
24. Oltvai, Z. N.; Milliman, C. L.; Korsmeyer, S. J. *Cell* **1993**, *74*, 609.
25. Gross, A.; McDonnell, J. M.; Korsmeyer, S. J. *Genes Dev.* **1999**, *13*, 1899.
26. Rowan, S.; Fisher, D. E. *Leukemia* **1997**, *11*, 45.
27. Thornberry, N. A.; Lazebnik, Y. *Science* **1998**, *281*, 1312.
28. Izban, K. F.; Wrone-Smith, T.; His, E. D.; Schnitzer, B.; Quevedo, M. E.; Alkan, S. *Am. J. Pathol.* **1999**, *154*, 1439.
29. Leng, Y.; Feng, Y.; Cao, L.; Gu, Z. P. *Acta Pharmacol. Sin.* **2001**, *22*, 155.
30. Zhu, X. H.; Shen, Y. L.; Jing, Y. K.; Cai, X.; Jia, P. M.; Huang, Y., et al. *J. Natl. Cancer Inst.* **1999**, *91*, 772.
31. Wright, S. C.; Schellenberger, U.; Wang, H.; Kinder, D. H.; Talhouk, J. W.; Larrick, J. W. *J. Exp. Med.* **1997**, *186*, 1107.
32. Zheng, X. L.; Sun, H. X.; Liu, X. L.; Chen, Y. X.; Qian, B. C. *Acta Pharmacol. Sin.* **2004**, *25*, 1090.